

Exotic quantum phase transitions in a Bose-Einstein condensate coupled to an optical cavity

Gang Chen

Department of Physics and Center of Theoretical and Computational Physics, The University of Hong Kong, Pokfulam Road, Hong Kong, China and Institute of Theoretical Physics, Shanxi University, Taiyuan 030006, China

Xiaoguang Wang

Zhejiang Institute of Modern Physics, Department of Physics, Zhejiang University, Hangzhou 310027, China

J.-Q. Liang

Institute of Theoretical Physics, Shanxi University, Taiyuan 030006, China

Z. D. Wang*

Department of Physics and Center of Theoretical and Computational Physics, The University of Hong Kong, Pokfulam Road, Hong Kong, China

(Received 18 March 2008; published 29 August 2008)

An extended Dicke model, which includes atom-atom interactions and a driving classical laser field, is established for a Bose-Einstein condensate inside an ultrahigh-finesse optical cavity. A feasible experimental setup with a strong atom-field coupling is proposed, where most parameters are easily controllable and thus the predicted a second-order superradiant-normal phase transition may be detected by measuring the ground-state atomic population. More intriguingly, *second-order* phase transition from the superradiant phase to the “Mott” phase is also revealed. In addition, a rich and exotic phase diagram is presented.

DOI: [10.1103/PhysRevA.78.023634](https://doi.org/10.1103/PhysRevA.78.023634)

PACS number(s): 03.75.Kk, 64.70.Tg, 42.50.Pq

As is known, a trapped Bose-Einstein condensate (BEC) may be used to generate a macroscopic quantum object consisting of many atoms that are in the same quantum state with a longer lifetime and can be excited by either deforming the trap or varying the interactions among atoms. Thus the BEC, as a distinct macroscopic quantum system, plays an important role in the in-depth exploration of both fundamental physics and quantum device applications of many-body systems [1]. In particular, an intriguing idea to combine the cavity quantum electrodynamics (QED) with the BEC has recently attracted significant interests both theoretically and experimentally as many exotic quantum phenomena closely related to both light and matter at ultimate quantum levels may emerge [2–9]. Very recently, a so-called strong coupling of a BEC to the quantized field of an ultrahigh-finesse optical cavity was realized experimentally [9], which not only implies that a challenging regime of cavity QED has been reached, where all atoms occupying a single mode of a matter-wave field can couple identically to the photon induced by the cavity mode, but also opens a wider door to explore a variety of different quantum phenomena associated with the cavity-mediated many-body physics of a quantum gas.

In this paper, we establish an extended Dicke model with controllable atom-atom interactions via Feshbach resonance [10] and a driving classical laser field under the two-mode approximation. A feasible experimental setup with controllable parameters including a collective strong atom-field coupling is proposed. We illustrate how to drive a well-known second-order superradiant-normal phase transition and how

to detect it experimentally. Remarkably, this superradiant phase transition was predicted in quantum optics many years ago, but has never been observed in experiments [11]. More intriguingly, a *second-order* superradiant-to-“Mott” phase transition is also revealed. This so-called Mott state is not a regular Mott state specified in lattices, as will be seen later. In addition, we also obtain a rich and exotic phase diagram covering phenomena from quantum optics to the BEC, which is attributed to the competition between the atom-atom and the atom-field interactions.

Our proposed experimental setup is depicted in Fig. 1. For an optical cavity with length $176 \mu\text{m}$ and the mode waist radius $27 \mu\text{m}$, we may choose the parameters of the cavity $(g_0, \kappa, \gamma) = 2\pi \times (10.6, 1.3, 3) \text{ MHz}$ [9], where g_0 is the maximum single atom-field coupling strength, and κ and γ are the amplitude decay rates of the excited state and the intracavity field, respectively. Such a choice implies that the system is in the strong-coupling regime, and thus the long-range coherence could be well established and the quantum dissipation effect may be safely neglected. Based on a pair of coupled Gross-Pitaevskii equations for the BEC with two levels $|F=1, m_f=-1\rangle$ ($|1\rangle$) and $|F=2, m_f=1\rangle$ ($|2\rangle$) of $5^2S_{1/2}$ [12] and, under the two-mode approximation, the total Hamiltonian for elastic two-body collisions with interaction potential of δ -functional type may be written as

$$\hat{H} = H_{\text{ph}} + H_{\text{at-ph}} + H_{\text{at}} + H_{\text{at-cl}} + H_{\text{at-at}} \quad (1)$$

with $H_{\text{ph}} = \omega a^\dagger a$ ($\hbar=1$ hereafter), $H_{\text{at}} = \omega_1 c_1^\dagger c_1 + (\omega_2 + \omega_{12}) c_2^\dagger c_2$, $H_{\text{at-at}} = \eta_1 c_1^\dagger c_1^\dagger c_1 c_1 / 2 + \eta_2 c_2^\dagger c_2^\dagger c_2 c_2 / 2 + \chi c_1^\dagger c_1 c_2^\dagger c_2$, $H_{\text{at-cl}} = \Omega [c_2^\dagger c_1 \exp(-i\varpi t) + c_1^\dagger c_2 \exp(i\varpi t)] / 2$, and $H_{\text{at-ph}} = \tilde{\kappa} (c_1^\dagger c_2 + c_2^\dagger c_1) (a^\dagger + a)$, where a is the annihilation operator of the cavity mode with frequency ω ; c_1 and c_2 are the annihilation

*zwang@hkuc.hku.hk

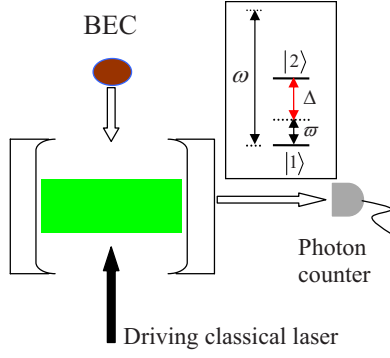


FIG. 1. (Color online) Schematic diagram of an experimental setup for a BEC of ^{87}Rb atoms coupled to a QED cavity. The BEC with two levels $|1\rangle$ and $|2\rangle$ is prepared in a time-averaged, orbiting potential magnetic trap. After moving the BEC into an ultrahigh-finesse optical cavity, an external controllable classical laser is applied to produce various transitions of the atoms between $|1\rangle$ and $|2\rangle$ states.

boson operators for $|1\rangle$ and $|2\rangle$, respectively; $\omega_l = \int d^3\mathbf{r} \{ \phi_l^*(\mathbf{r}) [-\nabla^2/2m_R + V(\mathbf{r})] \phi_l(\mathbf{r}) \}$ ($l=1,2$) with $V(\mathbf{r})$ being a single magnetic trapped potential of frequencies ω_i ($i=x,y,z$) and m_R being the atomic mass; ω_{12} is the atomic resonance frequency; $\eta_l = (4\pi\rho_l/m_R) \int d^3\mathbf{r} |\phi_l(\mathbf{r})|^4$ and $\chi = (4\pi\rho_{1,2}/m_R) \int d^3\mathbf{r} |\phi_1(\mathbf{r})|^2 |\phi_2(\mathbf{r})|^2$ with ρ_l and $\rho_{1,2}$ ($=\rho_{2,1}$) being the intraspecies and interspecies s -wave scattering lengths, respectively; $\Omega = 2\Omega_0 \int d^3\mathbf{r} \phi_2^*(\mathbf{r}) \phi_1(\mathbf{r})$ with Ω_0 being the Rabi frequency for the introduced classical laser with a driving frequency ϖ ; and $\tilde{\lambda} = \tilde{g} \int d^3\mathbf{r} \phi_2^*(\mathbf{r}) \phi_1(\mathbf{r}) = \tilde{g} \int d^3\mathbf{r} \phi_1^*(\mathbf{r}) \phi_2(\mathbf{r})$ with \tilde{g} being the interaction constant between the atom and the photon [13].

Under a unitary transformation $U = \exp(-i\varpi J_z t)$ with the condition $\varpi \ll \omega$ and using the Schwinger relations $J_x = (c_2^\dagger c_1 + c_1^\dagger c_2)/2$, $J_y = (c_1^\dagger c_2 - c_2^\dagger c_1)/2i$, and $J_z = (c_1^\dagger c_1 - c_2^\dagger c_2)/2$ with the Casimir invariant $J^2 = N(N/2 + 1)/2$, the Hamiltonian (1) can approximately be rewritten as

$$H = \omega a^\dagger a + \frac{\lambda}{\sqrt{N}} J_x (a^\dagger + a) + \omega_0 J_z + \Omega J_x + \frac{v}{N} J_z^2 \quad (2)$$

in the rotating frame, where $\lambda = 2\tilde{\lambda}\sqrt{N}$ denotes the collective coupling strength, $v = N[(\eta_1 + \eta_2)/2 - \chi]$ describes the atom-atom interactions including the repulsive ($v > 0$) and attractive ($v < 0$) interactions, and $\omega_0 = \omega_2 - \omega_1 + (N-1)(\eta_2 - \eta_1)/2 + \Delta$ with $\Delta = \omega_{12} - \varpi$ being the detuning. For a single trapped potential, we have $\omega_2 = \omega_1$ and consider only the case of $\rho_1 = \rho_2$, which has the advantages that it reduces the effects of fluctuations in the total atomic number and ensures a large spatial overlap of different components of the condensate wave function. Thus, the parameters v and ω_0 can further be reduced to $v = N(\eta_1 - \chi)$ and $\omega_0 = \Delta$. Equation (2) is a key result, which describes the collective dynamics for the composite system and has a rich phase diagram. Here we refer to this equation as an *extended Dicke model* since it contains an extra laser field term (the fourth one) and a “direct” atom-atom interaction term (the fifth one) in comparison with the standard Dicke model [11] and its generalized

version [14]. Note that the nonlinear atom-atom interaction was also considered in Ref. [9], where it is incorporated through the atom-laser-field coupling, with the overlap between the cavity mode and the BEC order parameter distribution being evaluated by numerically solving the Gross-Pitaevskii equation. As a result, the model established there is actually a kind of standard Dicke model.

A distinct property of the Hamiltonian (2) is that all parameters can be controlled independently. For example, the effective coupling strength λ can be manipulated by a standard technique. The effective Rabi frequency Ω and the detuning Δ depend on the experimentally controllable classical laser, and, in particular, the detuning Δ can vary continuously from red ($\Delta < 0$) to blue ($\Delta > 0$) detunings. The parameter v ranging from positive to negative is determined by the s -wave scattering lengths via the Feshbach resonance technique [10]. For $v=0$ ($\rho_{1,2} = \rho_1$) and $\Omega = \varpi = 0$, the Hamiltonian (2) is reduced to the standard Dicke model with a second-order superradiant phase transition at the critical point $\lambda_c = \sqrt{\omega\omega_0}$ [15]. It should be noticed that this important prediction has never been observed in experiments. The main difficulties are likely (i) all atoms can hardly interact identically with the same quantum field; (ii) the frequencies ω and ω_0 typically exceed the coupling strength λ by many orders of magnitude; (iii) it is hard to control the parameters as demanded. However, in our proposal, these difficulties could be completely overcome by using the currently available experimental techniques of BEC, as will readily be seen below.

To explore quantum phases and their transitions, we now investigate the ground-state properties of the Hamiltonian (2), which can approximately be dealt with by using the Holstein-Primakoff transformation, $J_\pm = b^\dagger \sqrt{N-b^\dagger b}$, $J_- = \sqrt{N-b^\dagger b} b$, and $J_z = (b^\dagger b - N/2)$ with $[b, b^\dagger] = 1$. Here we introduce two shifting boson operators $c^\dagger = a^\dagger + \sqrt{N}\alpha$ and $d^\dagger = b^\dagger - \sqrt{N}\beta$ with auxiliary parameters α and β to describe the collective behaviors of both the atoms and the photon [15]. With the help of the boson expansion method, the scaled ground-state energy is given by $E_0(\alpha, h)/N = \omega\alpha^2 - 2\lambda\alpha(h^2 - 1/2) + \Delta h\sqrt{1-h^2} + \Omega(h^2 - 1/2) + v h^2(1-h^2)$ with $h\sqrt{1-h^2} = \beta^2 - 1/2$ ($1/2 \leq h^2 \leq 1$). The critical points can be determined from the equilibrium condition $\partial[E_0(\alpha, h)/N]/\partial\alpha = 0$ and $\partial[E_0(\alpha, h)/N]/\partial h \times dh/d\beta = 0$, which leads to two equations: $\alpha = \lambda(\eta^2 - 1)/2\omega(\eta^2 + 1)$ and

$$2(u+v)\eta(1-\eta^2) + 2\Omega\eta(1+\eta^2) + \Delta(1-\eta^4) = 0, \quad (3)$$

where $\eta = h/\sqrt{1-h^2}$ and $u = \lambda^2/\omega$ are introduced as new parameters for convenience. The coefficient $(u+v)$ describes the intrinsic competition between the atom-atom and the atom-field interactions and gives rise to some exotic phase transitions predicted in the following.

Equation (3) contains the basic information about quantum phases and the corresponding transitions. As a benchmark, we first address the simplest case that there is no nonlinear interaction among atoms, namely, $v=0$ ($\rho_1 = \rho_{1,2}$). Figure 2 shows the scaled ground-state energy E_0/N and atomic population (or equivalently “magnetization”) m/N as a function of the detuning Δ for different Rabi frequencies (Ω). It can be seen clearly that in the limit $\Omega \rightarrow 0$ this system exhibits collective excitations of both the atom and the field

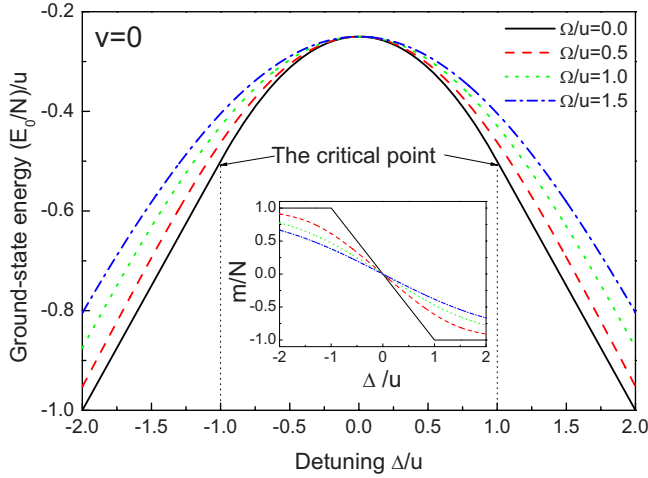


FIG. 2. (Color online) Scaled ground-state energy E_0/N and atomic population m/N (inset) versus the detuning Δ for different Rabi frequencies (Ω) at $v=0$.

with macroscopic occupations (i.e., $|m/N| < 1$ and $\langle a^\dagger a \rangle > 0$) for $-u < \Delta < u$, whereas there are no such excitations for $\Delta > u$ and $\Delta < -u$ (the solid black line). This interesting behavior typically indicates a second-order superradiant phase transition in quantum optics with the critical point $\Delta_c = \pm u$ [15]. Moreover, here we may achieve the condition that the order of magnitude of λ is the same as that of $\sqrt{\omega\Delta}$ by controlling the detuning of the classical laser. By controlling $\Omega/u \ll 1$ and evaluating a partial derivative of m with respect to Δ (or ω), if a peak is detected in the derivative, which becomes sharper and sharper if Ω becomes smaller and smaller, a second-order superradiant phase transition at $\Omega = 0$ is indicated, even though the transition disappears at a finite Rabi frequency Ω . In view of this, our proposed composite system with a controllable classical laser is a promising candidate for exploring cavity-induced superradiant phase transitions by measuring the ground-state atomic population via resonant absorption imaging [12].

On the other hand, the nonlinear interactions among atoms controlled by the Feshbach resonance technique play an important role for the ground-state properties. Figure 3 plots a zero-temperature phase diagram for the atom-atom interaction strength v and the detuning Δ with a Rabi frequency in the framework of the mean field. The table lists the corresponding ranges of the mean intracavity photon number $\langle a^\dagger a \rangle$, the atomic population $\langle J_z \rangle$, and the “susceptibility” $\partial \langle J_z \rangle / \partial v$ for three different quantum phases. In the case of a repulsive interaction ($v > 0$), the critical point becomes $\Delta_c = \pm(u+v)$, which implies that an effective atom-field interaction is enhanced, while in the weak-attractive-interaction case ($-u < v < 0$), the effective interaction is suppressed. However, the basic features of the superradiant phases remain. In particular, in the case of $v = -u$, this system exhibits a second-order phase transition from the superradiant to the Mott phases [red (leftmost vertical) line] [16]. The relevant physics can be intuitively understood as follows. In an optical cavity with $\omega \gg \lambda$, the cavity mode is only weakly or virtually excited, and the energy term $\omega a^\dagger a + (\lambda/\sqrt{N}) J_x$ ($a^\dagger + a$) is therefore nearly equal to $-u J_x^2/N$. If $v > -u$, the

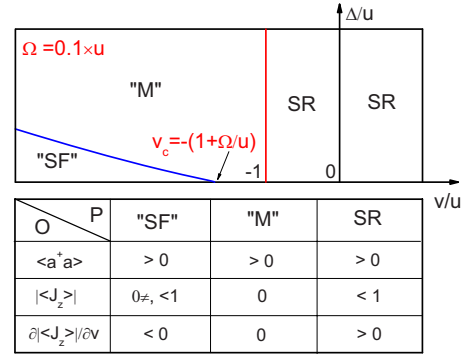


FIG. 3. (Color online) Zero-temperature phase diagram of the detuning Δ and the atom-atom interaction strength v with a Rabi frequency Ω . The blue (diagonal) line is determined by $\Delta = \pm [(u+v)^{2/3} - \Omega^{2/3}]^{3/2}$. Two interesting second-order phase transitions occur when crossing the red (leftmost vertical) and blue (diagonal) lines. Note that this phase diagram is symmetric with respect to $\Delta < 0$, simply because the Hamiltonian (2) is invariant under the transformation $\Delta = -\Delta$ and $J_z = -J_z$. The lower table denotes three different quantum phases. Here, SF is the “superfluid” phase, M the Mott phase, and SR the superradiant phase; P indicates phase, and O the order parameter.

ground-state properties are governed by the energy $-|u+v|J_x^2/N + \Delta J_z + \Omega J_x$. The effective potential in the Landau-Ginzburg theory is a double-well potential with photon-assisted Josephson tunneling, which means that this system is located in the superradiant phase. If $-u - \Omega < v < -u$, the energy $-|u+v|J_x^2/N + \Delta J_z + \Omega J_x$ is dominant and the corresponding effective potential is a single-well potential with no internal Josephson tunneling, leading to the same atomic numbers for the two levels ($m=0$); this may be referred to as the Mott phase [17]. Also, when v is decreased, a second-order phase transition from the Mott to the superfluid phase [blue (diagonal) line] occurs at the critical point $v_c = -u - (\Omega^{2/3} + \Delta^{2/3})^{3/2}$. In the so-called superfluid case, the effective potential is another double-well potential with internal Josephson tunneling induced by the attractive interaction [17]. It should be pointed out that these three different phases can be distinguished experimentally by measuring the atomic population $\langle J_z \rangle$ and the susceptibility $\partial \langle J_z \rangle / \partial v$. In the limit $\Omega \rightarrow 0$, this predicted second-order phase transition from the superradiant to the Mott phase becomes a direct transition from the superradiant to the superfluid phase with the same order at the critical point $v_c = -u$ and $\Delta = 0$.

Although the second-order superradiant phase transition disappears in the strong attractive interaction ($v < -u$), another interesting phase transition (from the phase with non-zero macroscopic occupation of level 1 to that of level 2) in the superfluid regime emerges when the detuning Δ changes from negative to positive (i.e., from red to blue detuning). Figure 4 shows the scaled atomic population m/N versus Δ for different Ω 's. We see that a *first-order* phase transition occurs at $\Delta = 0$ within the superfluid phase regime, which is simply the transition from the state $\langle J_z \rangle = m/N$ to the other state $\langle J_z \rangle = -m/N$, and moreover this first-order phase transition exists until $\Omega_c = |u+v|$ (red dashed line). For $\Omega = \Omega_c$, it becomes a *second-order* phase transition with the same criti-

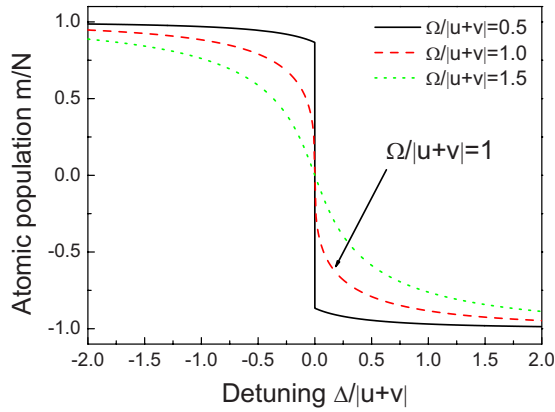


FIG. 4. (Color online) Scaled ground-state atomic population m/N versus the detuning Δ for different Rabi frequencies Ω when $v < -u$.

cal point. For $\Omega > \Omega_c$, no phase transition is seen when Δ is varied.

We now estimate the energy scales for the parameters in the Hamiltonian (2) to address the experimental feasibility. Under the two-mode approximation, the wave functions of the macroscopic condensate states for a single magnetic trap may roughly be approximated by $\phi_i(\mathbf{r}) = \pi^{-3/4} (d_x d_y d_z)^{-1/2} \exp[-(x^2/d_x^2 + y^2/d_y^2 + z^2/d_z^2)/2]$ with $d_x = \sqrt{1/m_R \omega_x}$, $d_y = \sqrt{1/m_R \omega_y}$, and $d_z = \sqrt{1/m_R \omega_z}$. Hence, the atom-atom interaction strength can be estimated by $v = N(\rho_1 - \rho_{1,2})/\sqrt{2\pi} d_x d_y d_z m_R$. For the typical values $(\omega_x, \omega_y, \omega_z) = 2\pi \times (290, 43, 277)$ Hz, $\rho_1 = 4.2$ nm, $\rho_{1,2} = 9.7$ nm, and $m_R = 1.45 \times 10^{-25}$ kg, the energy scale of v is about -0.238 MHz with $N = 5 \times 10^4$, which ensures that the error (the order of $1/\sqrt{N}$) for determining the ground-state properties by means of the Holstein-Primakoff transformation is very low. The effective coupling strength $\lambda = 2\tilde{\lambda}\sqrt{N} = 2.81 \times 10^4$ MHz for $\tilde{\lambda} = 2\pi \times 10$ MHz [9] is indeed in the strong-coupling regime. The energy scale for u is about 0.315 MHz for $\omega = 2.51 \times 10^9$ MHz [9], which can be adjusted by controlling the frequency of photon. These energy scales for u and v imply that the intrinsic competition between the atom-atom and atom-field interaction should be taken into account seriously in a BEC coupled to an optical

cavity. Also note that the aforementioned condition $\varpi \ll \omega$ is well satisfied once ϖ is tuned around ω_{12} , since $\omega_{12} \sim 6.8 \times 10^3$ MHz $\ll \omega$ [12].

Finally, we elaborate briefly on how to probe the predicted phase transitions experimentally. From the condition $\alpha = \lambda(\eta^2 - 1)/2\omega(\eta^2 + 1)$ with $\lambda = 2.81 \times 10^4$ MHz and $\omega = 2.51 \times 10^9$ MHz, we can immediately evaluate the maximum of the scaled mean intracavity photon number $\langle a^\dagger a \rangle/N$ and find it to be much less than the critical intracavity photon number $n_c = \gamma^2/2g_0^2 = 0.04$. Therefore, one is able to perform the transmission spectroscopy measurement with a weak probe laser to obtain the ground-state energy spectrum and atomic population since different quantum phases are, in general, characterized by their specific dispersion relations. The transmission (of this probe laser through the cavity) versus the detuning may be monitored and/or detected by counting photons out of the cavity. Only when the probe laser frequency matches a system in resonance, the corresponding transmission is anticipated [18].

Before concluding this paper, we wish to remark briefly the transition from the normal phase to the superradiant phase. In the derivation of Hamiltonian (1) and (2), the A^2 term (where A is the vector potential) has been neglected, as done in Refs. [14,15], etc., while the absence of the A^2 term seems to be crucial for the existence of quantum criticality in the present model, namely, the presence of a larger A^2 term in the model Hamiltonian may lead to vanishing of the criticality [19]. Although whether it could be omitted is still debatable, such a debate is not a serious concern in our proposal since the physical phases in the cavity QED systems considered here may not be sensitive to its omission [20].

In summary, we have established an extended Dicke model and designed an experimental setup with controllable parameters. An exotic phase diagram has been obtained, that covers various phenomena from quantum optics to the BEC and reveals particularly several quantum phase transitions.

We thank S. L. Zhu, Y. Li, D. L. Zhou, L. B. Shao, and Z. Y. Xue for helpful discussions. This work was supported by the RGC of Hong Kong under Grants No. HKU7051/06P, No. HKU7044/08P, and No. HKU-3/05C, the URC fund of HKU, and the NSFC under Grants No. 10429401, No. 10775091, and No. 10704049.

[1] I. Bloch, *Nat. Phys.* **1**, 23 (2005).
 [2] C. Maschler and H. Ritsch, *Phys. Rev. Lett.* **95**, 260401 (2005); I. B. Mekhov, C. Maschler, and H. Ritsch, *Nat. Phys.* **3**, 319 (2007); *Phys. Rev. Lett.* **98**, 100402 (2007); *Phys. Rev. A* **76**, 053618 (2007); H. Zoubi and H. Ritsch, *ibid.* **76**, 013817 (2007).
 [3] J. Larson, B. Damski, G. Morigi, and M. Lewenstein, *Phys. Rev. Lett.* **100**, 050401 (2008); J. Larson, S. Fernandez-Vidal, G. Morigi, and M. Lewenstein, *New J. Phys.* **10**, 045002 (2008); J. Larson, G. Morigi, and M. Lewenstein, *Phys. Rev. A* **78**, 023815 (2008).
 [4] G. Chen, Z. D. Chen, and J.-Q. Liang, *Europhys. Lett.* **80**,

40004 (2007); J. M. Zhang, W. M. Liu, and D. L. Zhou, *ibid.* **77**, 033620 (2008); D. Nagy, G. Szirmai, and P. Domokos, *Eur. Phys. J. D* **48**, 127 (2008); A. B. Bhattacharjee, *Opt. Commun.* **281**, 3004 (2008).
 [5] A. Öttl, S. Ritter, M. Köhl, and T. Esslinger, *Phys. Rev. Lett.* **95**, 090404 (2005); T. Bourdel, T. Donner, S. Ritter, A. Öttl, M. Köhl, and T. Esslinger, *Phys. Rev. A* **73**, 043602 (2006).
 [6] S. Slama, S. Bux, G. Krenz, C. Zimmermann, and P. W. Courteille, *Phys. Rev. Lett.* **98**, 053603 (2007); S. Slama, G. Krenz, S. Bux, C. Zimmermann, and P. W. Courteille, *Phys. Rev. A* **75**, 063620 (2007).
 [7] S. Gupta, K. L. Moore, K. W. Murch, and D. M. Stamper-

- Kurn, Phys. Rev. Lett. **99**, 213601 (2007); K. W. Murch, K. L. Moore, S. Gupta, and D. M. Stamper-Kurn, e-print arXiv:0706.1005 (2007).
- [8] Y. Colombe, T. Steinmetz, G. Dubois, F. Linke, D. Hunger, and J. Reichel, Nature (London) **450**, 272 (2007).
- [9] F. Brennecke, T. Donner, S. Ritter, T. Bourdel, M. Köhl, and T. Esslinger, Nature (London) **450**, 268 (2007).
- [10] S. Inouye, M. R. Andrews, J. Stenger, H.-J. Miesner, D. M. Stamper-Kurn, and W. Ketterle, Nature (London) **392**, 151 (1998).
- [11] R. H. Dicke, Phys. Rev. **93**, 99 (1954).
- [12] M. R. Matthews, D. S. Hall, D. S. Jin, J. R. Ensher, C. E. Wieman, E. A. Cornell, F. Dalfovo, C. Minniti, and S. Stringari, Phys. Rev. Lett. **81**, 243 (1998).
- [13] M. G. Moore, O. Zobay, and P. Meystre, Phys. Rev. A **60**, 1491 (1999).
- [14] Y. Li, Z. D. Wang, and C. P. Sun, Phys. Rev. A **74**, 023815 (2006).
- [15] C. Emary and T. Brandes, Phys. Rev. E **67**, 066203 (2003); G. Chen, Z. D. Chen, and J.-Q. Liang, Phys. Rev. A **76**, 045801 (2007).
- [16] The first-order derivative of the ground-state energy with respect to v , is continuous at $v=-u$, but its second-order derivative has discontinued at the same point.
- [17] M. Jääskeläinen and P. Meystre, Phys. Rev. A **71**, 043603 (2005).
- [18] A. Öttl, S. Ritter, M. Köhl, and T. Esslinger, Rev. Sci. Instrum. **77**, 063118 (2006).
- [19] K. Rzażewski, K. Wódkiewicz, and W. Zakowicz, Phys. Rev. Lett. **35**, 432 (1975); I. Bialynicki-Birula and K. Rzażewski, Phys. Rev. A **19**, 301 (1979); M. Orszag, J. Phys. A **10**, 1995 (1977).
- [20] F. Dimer, B. Estienne, A. S. Parkins, and H. J. Carmichael, Phys. Rev. A **75**, 013804 (2007).